

1 **FIGURE S6. Characteristics of *Rickettsia* Ankyrin Repeat 2 (RARP-2) proteins and**  
2 **related ankyrin repeat containing proteins.**

3 **(A)** Comparison of the domain architecture for *Rickettsia* RARP-2 proteins (*R. typhi* str.  
4 Wilmington as an exemplar, NCBI acc. no. AAU04065) and the ANK repeat-containing  
5 protein DFA\_04436 (XP\_004360169) of the cellular slime mold *Cavenderia fasciculata*  
6 (Eumycetozoa; Dictyostelia; Acytosteliales). **(B)** Sequence logos (190) constructed to  
7 illustrate the conservation between ANK repeats within *R. typhi* RARP-2 and D  
8 DFA\_04436 and between the two models. Repeats were manually stacked and  
9 visualized with AliView 1.28.1 (207). Amino acid coloring is described in the **FIG. 3**  
10 legend. **(C)** Structure of the *R. typhi* RARP-2 C-terminal ANK repeat domain. **(left)**  
11 Alignment of the entire ANK repeat-containing domains between *R. typhi* RARP-2 and  
12 *C. fasciculata* DFA\_04436. Alignment constructed using MUSCLE (189) (default  
13 parameters). Helices above ANK repeats are derived from the conserved ANK repeat  
14 structure (118). Red sequence illustrates the fourth ANK repeat present in RARP-2 of *R.*  
15 *typhi* str. TH1527 (AFE54444), *R. typhi* str. B9991CWPP (AFE55282) and the  
16 laboratory strain named “Wilmington” that differs from AAU04065 and remains  
17 unpublished (58). **(right)** Prediction of entire RARP-2 structure using Alphafold (197,  
18 198). Additional ANK-like folds flanking the 11 ANK repeats predicted by comparative  
19 analyses are noted with question marks. **(D)** Summary of divergent RARP-2 (dRARP-2)  
20 proteins. N-terminal protease domains from each of the six sequences in the outer circle  
21 were used as a query in BlastP searches and determined to have greater similarity to a  
22 cohort (number in parentheses and size of dot) or itself only (Pyropec, or *Rickettsia*  
23 endosymbiont of *Pyrocoelia pectoralis*, a MAG from Davison *et al.* (73)) versus other

- 24 query sequences or any RARP-2 protein (center). All sequence information is provided
- 25 in [Table S2](#).

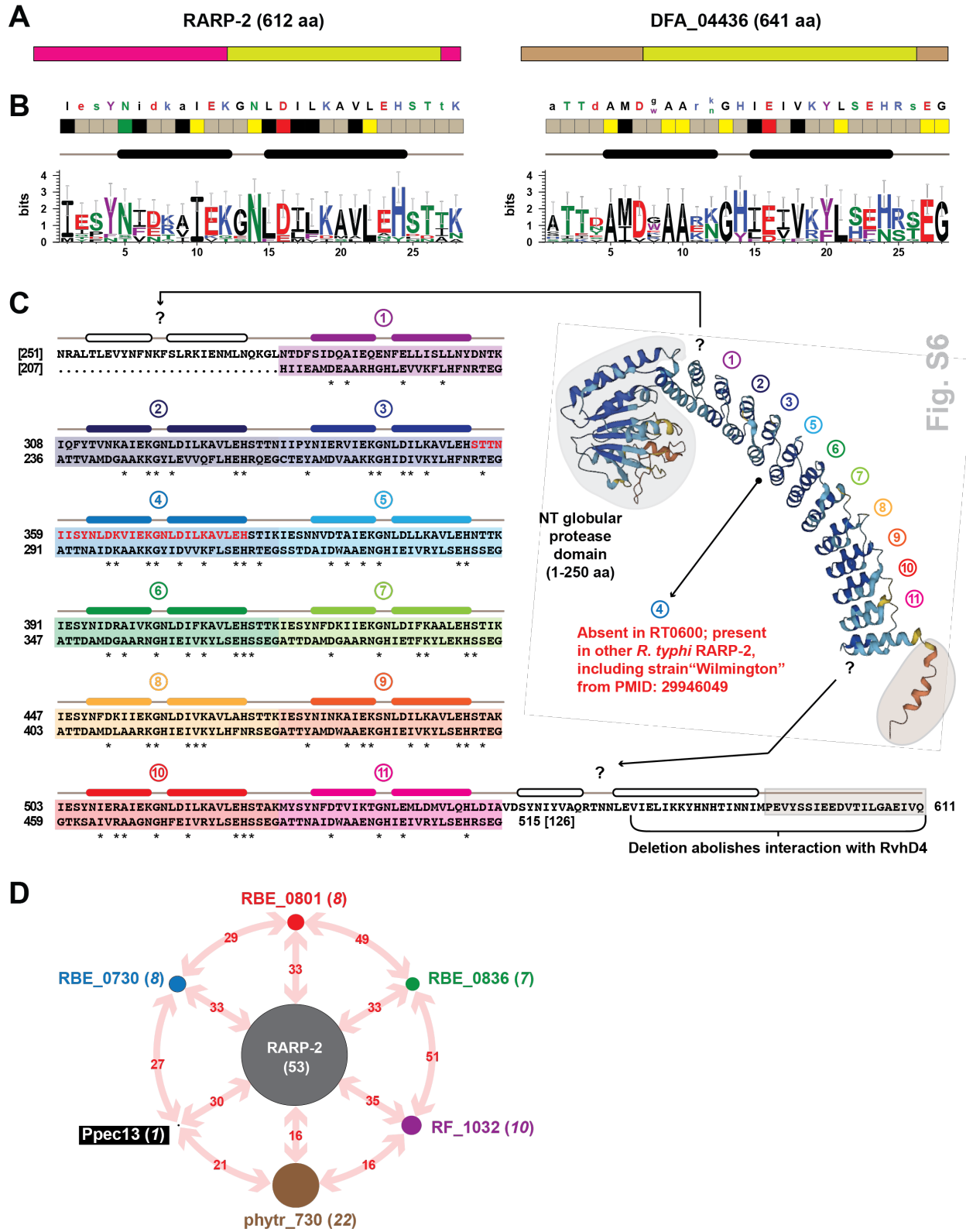


Fig. S6

**FIGURE S7. Phylogenomics analyses of candidate REMs (cREM-1-cREM-5).**

Protein information is provided in **Table S2**. All alignments done with MUSCLE (default parameters) (189) with conservation analyzed using WebLogo (190). Amino acid coloring is described in the **FIG. 3** legend. Black boxes provide short names for MAGs from Davison *et al.* (73). **(A)** cREM-1 proteins are minimized in architecture relative to ancestral forms. Proteins with high similarity to RT0435 (cREM-1) are mostly conserved in *Rickettsia* genomes yet highly diverse (gray), sometimes duplicated and tandemly arrayed (red) and often components of larger modular proteins (cREM-1d). Inset illustrates cREM-1 similarity to tandem repeats in the scrub typhus effector OtDUB (CAM80065), which carries multiple eukaryotic-like domains (5, 124, 203) (described in **FIG. 7**). For brevity, alignment of a small conserved region shared across OtDUB repeat 1 (383-406), OtDUB repeat 2 (645-668), Blapp1 HJD67197, and Blapp1 HJD67198 is shown. Phylogeny estimation of 102 cREM-1 proteins indicates diversification of larger cREM-1 domain modular proteins and streamlining to a single cREM-1 protein in most *Rickettsia* genomes. Alignment was not masked (1544 total sites, 38.34% invariant). A maximum likelihood-based phylogeny was estimated with PhyML (185), using the Smart Model Selection (186) tool to determine the best substitution matrix and model for rates across aa sites (VT +G+F). Branch support was assessed with 1,000 pseudo-replications. Log likelihood of tree: -34728.6. **(B)** cREM-2 proteins diversified from an ancient gene duplication. Proteins with high similarity to RT0352 (cREM-a, red) and RT0351 (cREM-2b, light blue) are tandemly arrayed and mostly conserved in *Rickettsia* genomes, yet highly diverse from ancient forms (cREM-2d). Inset illustrates the conserved central region of cREM-2 proteins. Estimated phylogeny indicates cREM-2b

52 proteins are more divergent from cREM-2d proteins. Alignment was not masked (973  
53 total sites, 43.4% invariant). Phylogeny estimated as described in panel **A** (final model  
54 LG +G). Branch support was assessed with 1,000 pseudo-replications. Log likelihood of  
55 tree: -25322.17. **(C)** cREM-3 proteins are highly conserved and present in other  
56 proteobacterial assemblies. These proteins are typically annotated as Pfam PF10877  
57 (DUF2671: restricted to *Rickettsia* spp.). This sequence logo is for 107 non-redundant  
58 proteins obtained from searches against 'Rickettsiales', with proteins aligned using  
59 MUSCLE (default parameters). A more complete list of proteins is found in **Table S2**,  
60 though more sequences are likely retrievable using HMMER searches. At bottom, a  
61 pairwise alignment between *R. typhi* RT0206 and the most divergent subject retrieved  
62 from a BlastP search excluding 'Rickettsiales' is shown (hypothetical protein  
63 B7X02\_01410 from Rhodospirillales bacterium 12-54-5, OYW13786.1). These proteins  
64 are 30% identical over the match shown. The residues noted with arrows in the  
65 sequence logo are shown over the pairwise alignment and below with a structure for *R.*  
66 *typhi* RT0206 predicted with Alphafold (197, 198). **(D)** cREM-4 proteins harbor a  
67 conserved pentapeptide repeat (PR). Schema shows alignment of 82 non-redundant  
68 cREM-4 proteins with illustration of the PR consensus sequence at top (208). A small  
69 conserved motif (inset) was also identified. **(E)** cREM-5 and cREM-5p have conserved  
70 central regions that lack similarity to proteins outside of *Rickettsia* and *Tisiphia*  
71 genomes. **(F)** One copy of cREM-5p from the RiClec (Endosymbiont of *Cimex*  
72 *lectularius*) genome is found on a RAGE transposon. General schema and annotation of  
73 RAGE genes follows previous reports (91, 92, 133).

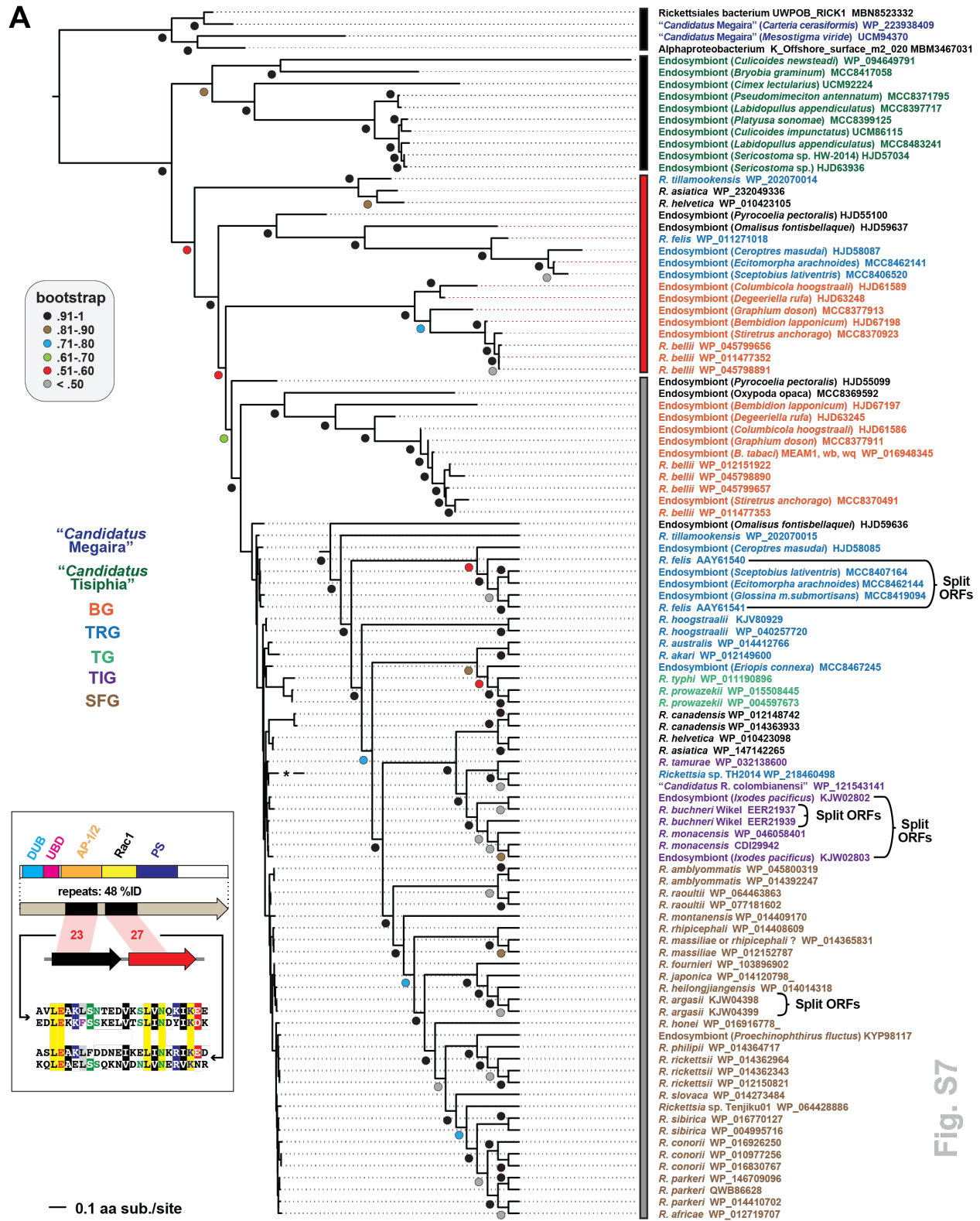


Fig. S7

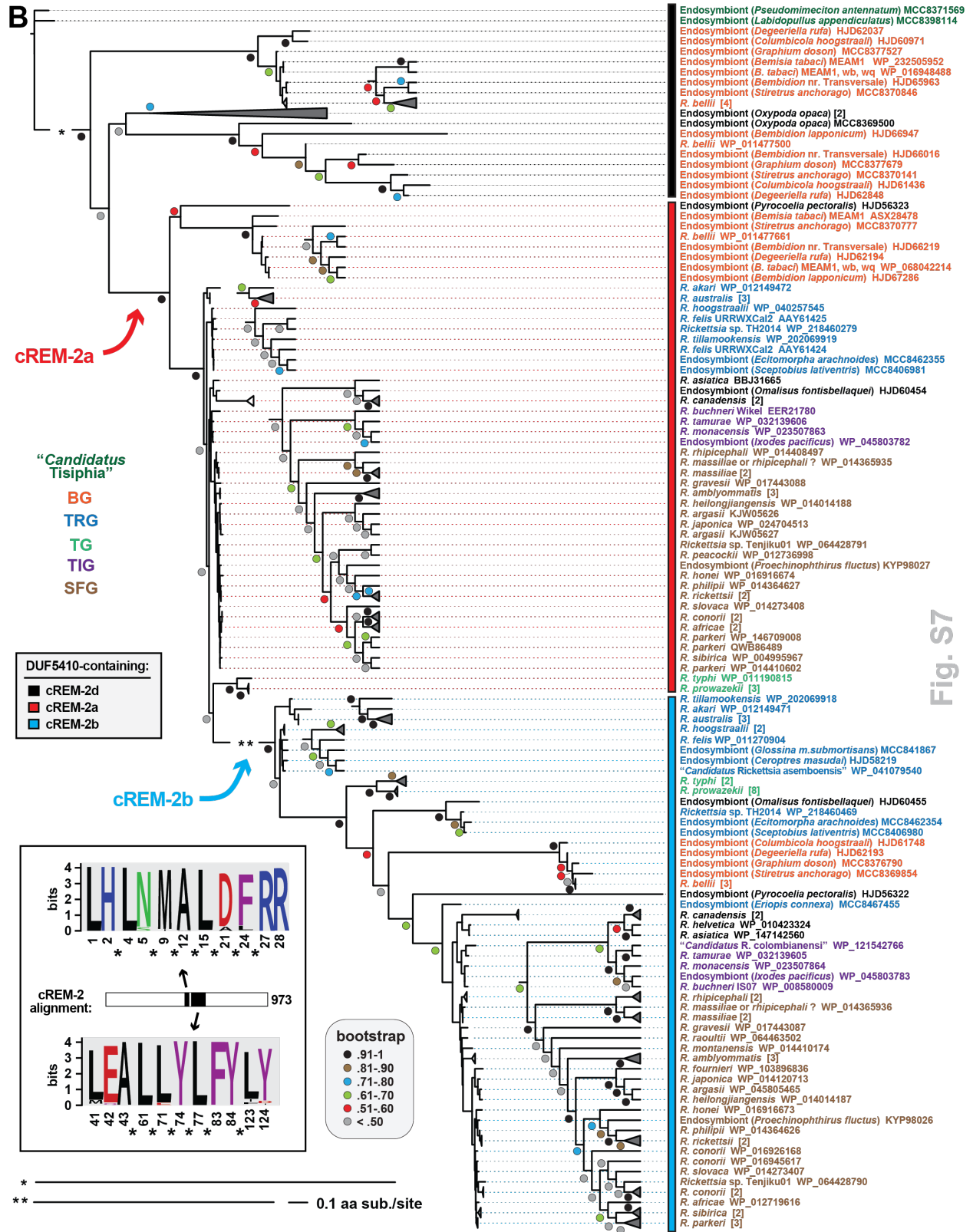


Fig. S7





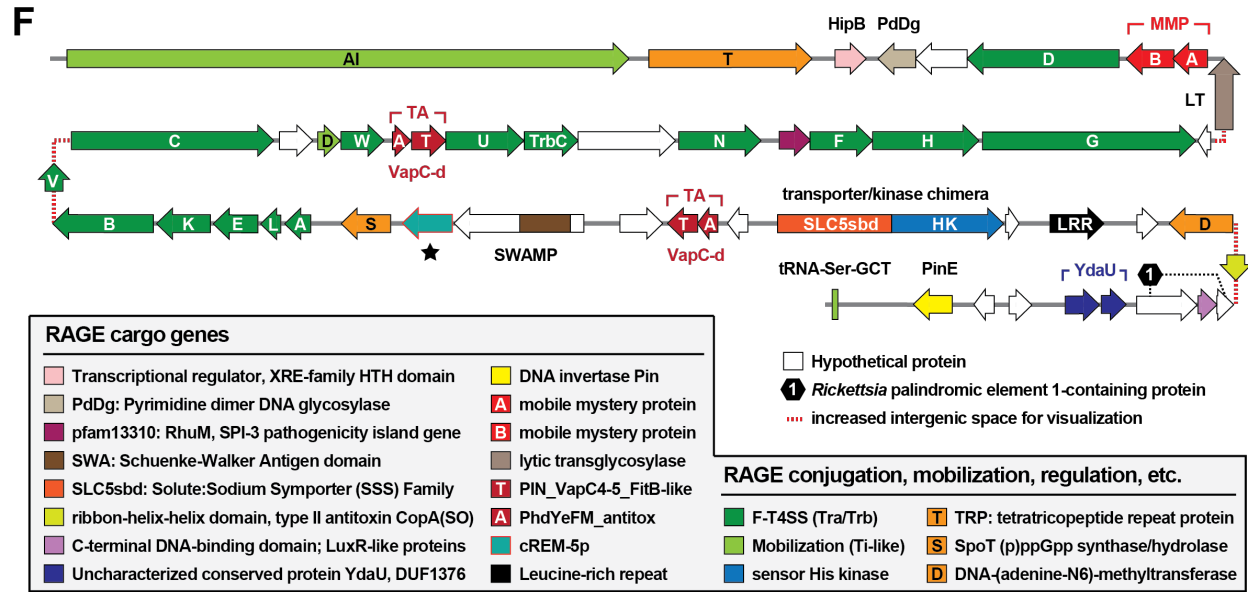


Fig. S7

80  
81

82 **FIGURE S8. Discovery of novel RickA architecture.** Black boxes provide short  
83 names for 29 MAGs from Davison *et al.* (73). Amino acid coloring is described in the  
84 **FIG. 3** legend. Sequence logos constructed with WebLogo 3 (190). Sequence  
85 information in **Table S2**. **(A)** General architecture of RickA proteins deduced from an  
86 alignment of 71 non-redundant sequences using MUSCLE (189) (default parameters).  
87 Consensus sequences for the WH2 (divided into two types based on one or two motifs)  
88 are shown at top, with divergent motifs illustrated. The remaining graphics illustrate the  
89 differences between *Tisiphia* and *Rickettsia* RickA C-terminal regions (summarized in  
90 the yellow ellipse). **(B)** Identification of a novel N-terminal repeat sequence in all RickA  
91 proteins. The repeat was identified by assessing within-protein BlastP matches, which  
92 revealed ~34 %ID between ~95 aa regions flanking the G-actin-binding domain  
93 (depicted in schema at top). Two examples are shown for a *Tisiphia* and *Rickettsia*  
94 repeat alignment, with secondary structure predictions indicating high conservation  
95 between repeats (199) . A comparison of the repeats R and R' all 71 non-redundant  
96 sequences is shown at bottom, with residues showing conservation in amino acid type  
97 (hydrophobicity, charge, aromaticity) shaded tan. This collectively illustrates that each  
98 RickA protein has greater within-repeat similarity than across-protein repeat similarity  
99 yet is constrained in overall amino acid type.

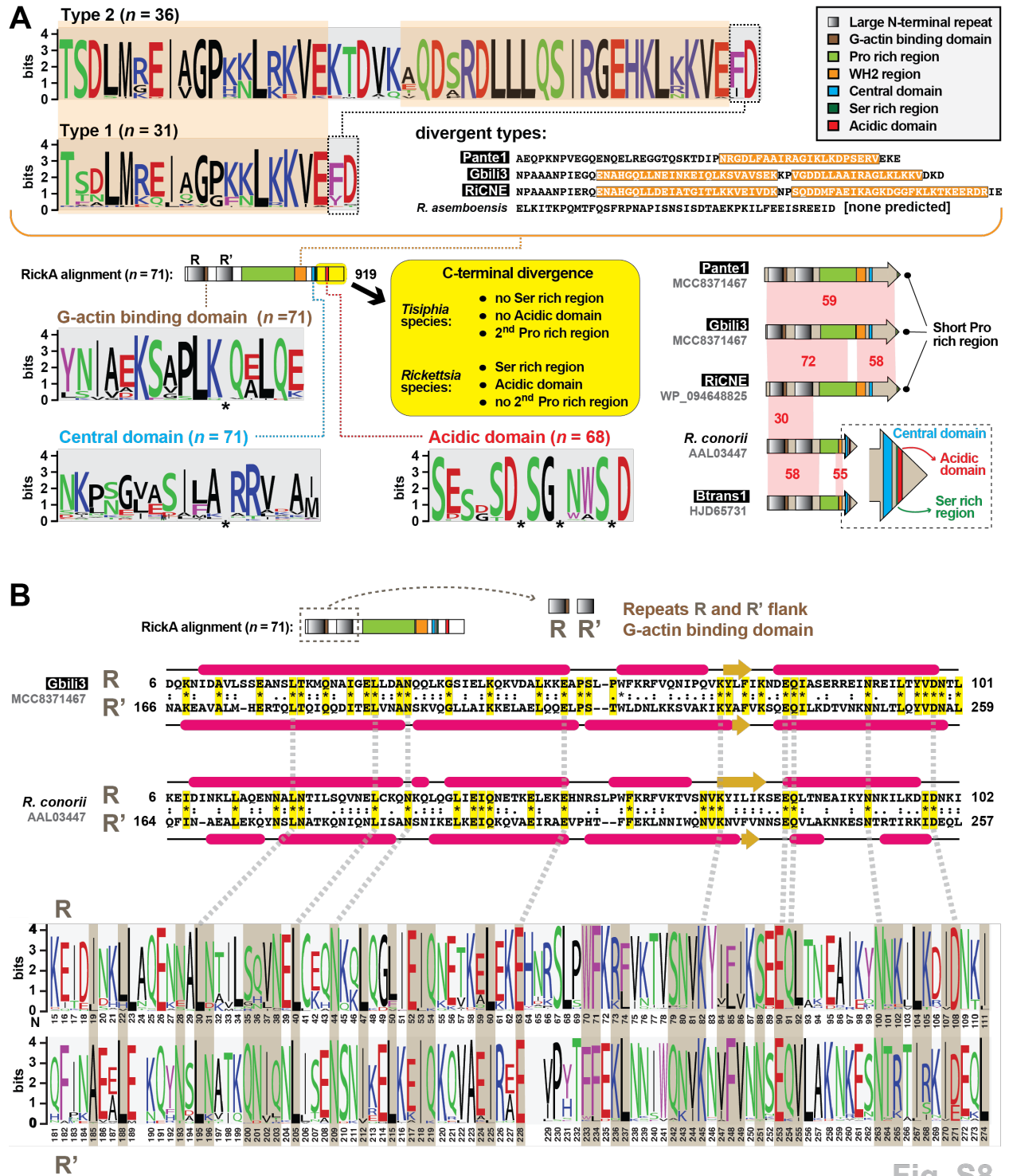


Fig. S8

103 **FIGURE S9. CDI-like/Rhs-like C-terminal toxin/antidote (CRCT/CRCA) modules**  
104 **occur in diverse rickettsial genomes.** Black boxes provide short names for 29 MAGs  
105 from Davison *et al.* (73). Sequence information in **Table S2.** **(A)** Comparison of the  
106 *Cupriavidus taiwanensis* str. DSM 17343 CdiA/I module to several rickettsial large  
107 modular toxins, as well as select rCRCT/CRCA-3a modules. Domains were predicted  
108 with SMART (191). Amino acid similarity (%ID, red shading) was assessed using Blastp.  
109 **(B)** Structural analysis of a rCRCT/CRCA-3a module. **(top)** Alignment of *C. taiwanensis*  
110 CdiA with eight rickettsial rCRCT-3a toxins. Amino acid coloring is described in the **FIG.**  
111 **3** legend. Structural information from *C. taiwanensis* CdiA (PDB:5T87) (209) is provided  
112 at top. Alignment performed using MUSCLE with default settings (189). **(bottom)**  
113 Modeling with Phyre2 (195) of six rCRCT-3a toxins to the CdiA-CT toxin structure of *C.*  
114 *taiwanensis* CdiA (PDB:5T87). All threading was done with >95% confidence. The  
115 *Jidaibacter* proteins were too divergent to model. Inset: while the *C. taiwanensis* module  
116 was solved as a co-complex (209), Phyre2 modeling could not thread rickettsial rCRCA-  
117 3a to the antidote CdiI within the TA co-complex. The best model (46.3% confidence,  
118 12% ID) for *R. tamurae* rCRCA-3a was to the structure of *Drosophila melanogaster*  
119 MAST/Orbit N-terminal domain PDB:4G3A (210), indicating a similar helical bundle and  
120 similar topology as *C. taiwanensis* CdiI.

121

122

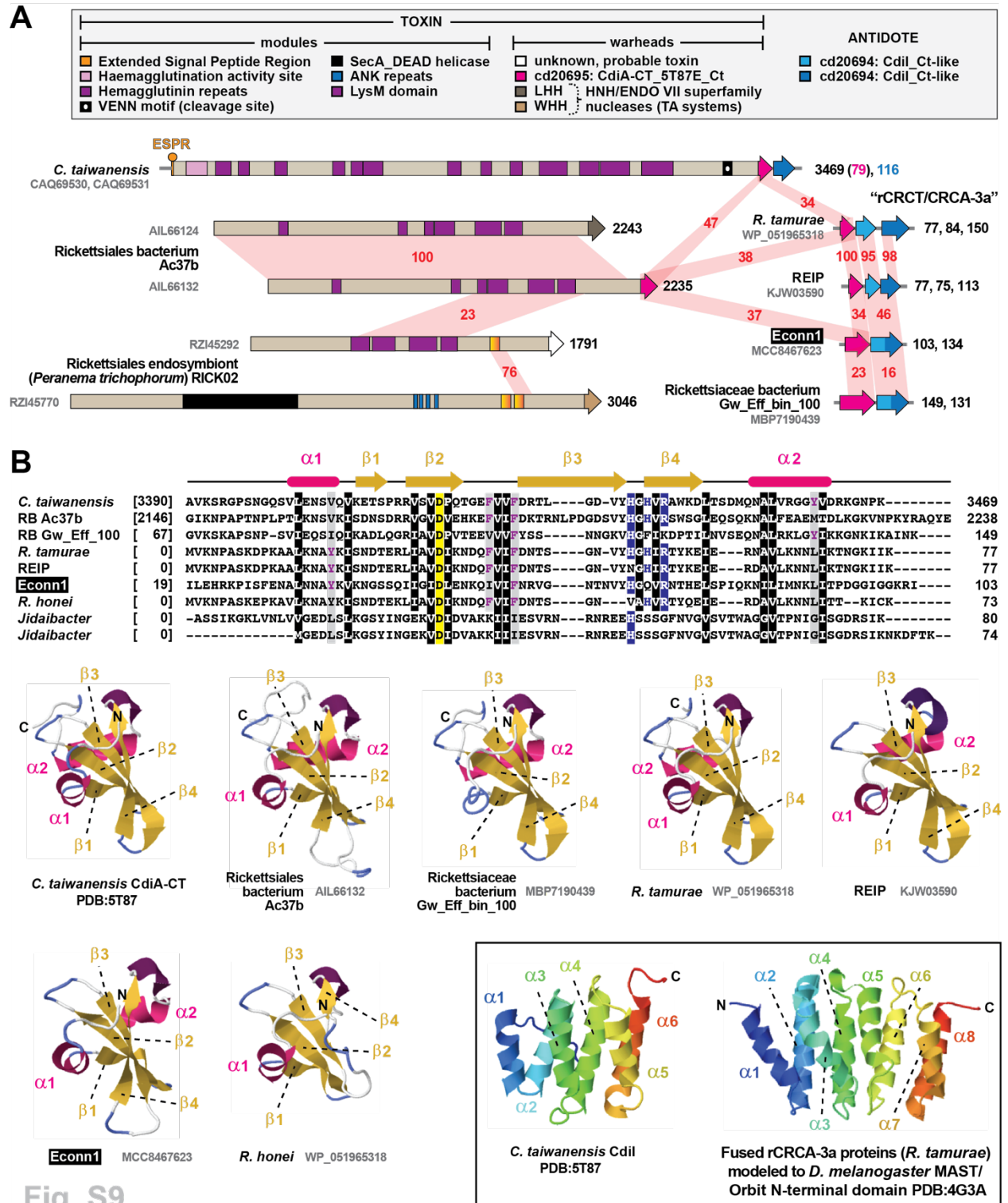
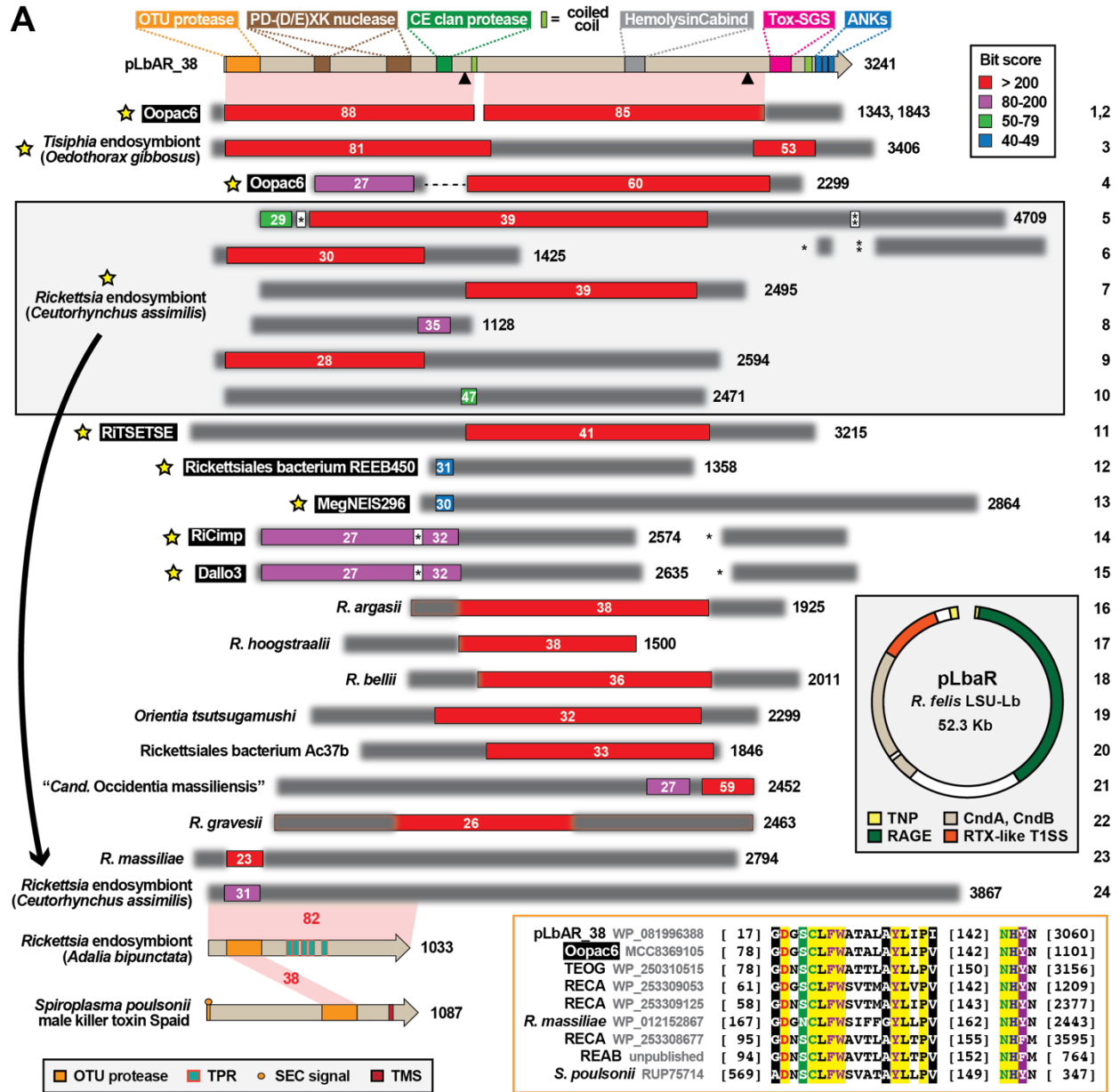


Fig. S9

125 **FIGURE S10. Identification of MAG proteins that have characteristics of**  
126 **reproductive toxins.** Black boxes provide short names for 29 MAGs from Davison *et*  
127 *al.* (73). Sequence information in **Table S2**. [NOTE: The *Rickettsia* endosymbiont of  
128 *Oedothorax gibbosus* (NZ\_OW370493) and *Rickettsia* endosymbiont of *Ceutorhynchus*  
129 *assimilis* (NZ\_OU906081) assemblies were not included in our other analyses, as  
130 manuscripts supporting these assemblies were not published. We included them in this  
131 analysis due to their relevance to reproductive parasitism (RP) in *Rickettsia* species].  
132 **Top**, architecture of the modular protein pLbAR\_38, which is carried on plasmid pLbAR  
133 of *Rickettsia felis* str. LSU-Lb (gray inset) (92). Black triangles, proprotein convertase  
134 cleavage sites (211). We refer to this protein and its adjacent predicted antidote (not  
135 shown) as a CndA/B module (174), as the toxin encodes nuclease (CinB) and  
136 deubiquitinase (CidB) domains similar to RP toxins of certain wolbachiae that cause  
137 cytoplasmic incompatibility in arthropod hosts (168–171). We previously showed that  
138 pLbAR\_38 shares similarity to a diverse assemblage of proteins from a narrow range of  
139 obligate intracellular bacteria, some of which are known reproductive parasites (5).  
140 Here, the remaining schema shows the result of a Blastp search against the NCBI nr  
141 database using pLbAR\_38 (coordinates 1-3048, which excludes the ankyrin repeats) as  
142 the query (inset, color key for alignment scores). NOTE: each subject (numbered 1-24  
143 at right) represents a distinct protein architecture, yet in some cases multiple similar  
144 proteins can be found for closely related species and strains). Yellow stars, novel RP  
145 toxins identified since our prior report (5). Matches for wolbachiae, *Cardinium* species  
146 (Bacteroidetes), *Diplorickettsia* species (*Gammaproteobacteria*), and *Rickettsiella*  
147 species (*Gammaproteobacteria*) are not shown to emphasize novel findings in

148 Rickettsiaceae. White numbers indicate % identity across significant alignments.  
149 Subjects missing internal sequence relative to pLbAR\_38 (no. 4) are joined by dashed  
150 lines; subjects with large insertions relative to pLbAR\_38 are adjusted accordingly (nos.  
151 5, 14, and 15). Blurred-out regions within subjects depict sequences with no significant  
152 matches to pLbAR\_38. Six proteins for the *Rickettsia* endosymbiont of *Ceutorhynchus*  
153 *assimilis* are boxed, with the arrow pointing to a seventh protein that is directly  
154 compared to a protein from the *Rickettsia* endosymbiont of *Adalia bipunctata*  
155 (unpublished assembly), which contains the ovarian tumor (OTU) cysteine protease  
156 (Pfam OTU, PF02338) domain also found in the Spaid male-killer toxin of *Spiroplasma*  
157 *poulsonii* sp. (172). Inset, alignment of the OTU protease domains of select bacteria:  
158 TEOG, *Tisiphia* endosymbiont of *Oedothorax gibbosus*; RECA, *Rickettsia* endosymbiont  
159 of *Ceutorhynchus assimilis*; REAB, *Rickettsia* endosymbiont of *Adalia bipunctata*.  
160 Amino acid coloring is described in the **FIG. 3** legend.  
161  
162



163  
164

Fig. S10